subjected to a fixed strain, the stress within the tissue decreases, *i.e.* it experiences stress relaxation. Similarly, when a tissue is subjected to a fixed stress its strain will continue to increase, *i.e.* it exhibits creep.

Recent experiments have used synchrotron radiation to investigate the orientation of collagen fibrils in skin and perimysium (muscle connective tissue) [7]. In both tissues, the initial application of load leads to fibrils tending to reorient in the direction of applied load. However, there was no detectable change in fibril orientation during either creep or stress relaxation. These results indicate that simple geometric models are inadequate to explain the viscoelastic properties of ECM. This result is expected for stress relaxation, where the overall dimensions of the tissue do not change, and is consistent with X-ray diffraction patterns of intervertebral disc [4] and ligaments [5] showing fixed fibril orientations over a period of about 30 min at fixed strains. However, the results of creep experiments are more surprising and merit further investigation.

Preliminary experiments are also being performed on the response of the collagen fibril network of uterine cervix to creep (in collaboration with Mr S.J.Wilkinson). These experiments are being performed on rat tissue which provides an established model for the changes which occur in the human cervix during labour [6]. The creep rate of the cervix increases at term, allowing it to dilate so that the neonate can pass through. Furthermore, this change in mechanical properties is accompanied by a change in NMR relaxation times [14] which may explain the changes apparent in MR images of human patients. Understanding the relationship between structure and mechanical properties of the the rat cervix may then be a step in relating the appearance of the human cervix in MR images to its properties and, hence, to the diagnosis of a cervix which changes its mechanical properties too early in pregnancy or not at all.

References

[1] D.W.L. Hukins, R.M. Aspden. In *Material Properties and Stress Analysis in Biomechanics*, A.L. Yettram (ed.), pp. 44-59, Manchester University Press, Manchester, 1989.

[2] R.M. Aspden, D.W.L. Hukins. In *Material Properties and Stress Analysis in Biomechanics*, A.L. Yettram (ed.), pp. 109-122, Manchester University Press, Manchester, 1989.

[3] D.S. Hickey, J.I. Phillips, D.W.L. Hukins. *British Journal of Urology* **54**, 556-561 (1982).

[4] D.W.L. Hukins. In *Biology of the Intervertebral Disc*, vol. 1, P. Ghosh (ed.), pp. 1-37, CRC Press, Boca Raton, 1988.

[5] D.W.L. Hukins, M.C. Kirby, T.A. Sikoryn, R.M. Aspden, A.J. Cox. *Spine* **15**, 787-795 (1990).

[6] R.M. Aspden. In *Connective Tissue Matrix*, part 2, D.W.L. Hukins (ed.), pp. 199-228, Macmillan, London, 1990.

[7] P.P. Purslow, D.W.L. Hukins. International Biomechanics Conference, Amsterdam, 1994.

[8] M.C. Kirby, R.M. Aspden, D.W.L. Hukins. *Journal of Applied Crystallography* **21**, 929-934 (1988).

[9] J.A. Klein, D.W.L. Hukins, *Biochimica et Biophysica Acta* **717**, 61-64 (1982).

[10] K.J. Mathias, J.R. Meakin, A. Heaton, M.W. Brian, S. Mierendorff, R.M. Aspden, J.C. Leahy, D.W.L. Hukins. In *NAFEMS World Congress*, in press.

[11] A.J. Fennell, A.P. Jones, D.W.L. Hukins. *Spine*, in press.

[12] A.D. Holmes, D.W.L. Hukins. *Medical Engineering and Physics* **18**, 99-104 (1996).

[13] J.C. Leahy, D.W.L. Hukins. *Journal of Back and Musculoskeletal Rehabilitation*, in press.

[14] J. Blacker, M.A. Foster, R.M. Aspden. British Institute of Radiology Meeting, Birmingham,

Diffraction by Disordered Fibres

R. P. Millane and W. J. Stroud

Whistler Center for Carbohydrate Research and Computational Science and Engineering Program, Purdue University, West Lafayette, Indiana 47907-1160, U.S.A.

Introduction

Diffraction patterns from some polycrystalline fibres contain sharp Bragg reflections at low resolution, giving way to continuous layer line intensities at high resolution [1,2]. Such specimens are essentially polycrystalline, but the packing of the molecules in the crystallites is disordered. Accurate structure

determination using data from such diffraction patterns requires that the effects of disorder on the diffracted intensities be included in a rigorous manner. Towards this end, we have developed models of disordered polycrystalline fibres and their diffraction properties [3-7], which we summarise here.

The approach we adopt involves construction of statistical models of disordered crystallites, and calculation of resulting diffraction patterns. Disorder is described in terms of probability density functions that describe perturbations of the crystalline structure away from ideal order, and the diffraction from a fibre is calculated as an ensemble average over the imperfect crystallites. An alternative approach is to build representative crystallites based on appropriate intermolecular potentials and average the diffraction over many such realisations. Although this approach may be useful for some simple systems, for more complex systems it has the disadvantage that the results depend on knowing the relevant potentials quite accurately, and it is enormously expensive computationally. Our approach is to describe the overall distortions in the crystal lattice (which are the primary determinants of the diffraction) while ignoring the details of the particular interactions that give rise to these. The advantage of this approach is that it is generally applicable, and analytical expressions can be obtained that allow efficient calculation of diffraction patterns.

It is convenient to regard disorder as having two components, referred to as *lattice disorder* and *substitution disorder*. Lattice disorder consists of deviations in the positions of the molecules from those in an average lattice. The molecules are treated as rigid bodies, so that lattice disorder consists of distortions of a two-dimensional lattice into three-dimensional space. Substitution disorder consists of variations in the dispositions of the molecules at each lattice site, which in our case consists of rotations of the molecules about their long axes, and variations in their direction ("up" or "down"). Lattice and substitution disorder are assumed to be independent of each other.

The layer line intensities diffracted from an ensemble of disordered crystallites can be written as

$$I_l(R) = \left\langle \left\langle I(R, \psi, Z = l/c) \right\rangle_d \right\rangle_\psi \qquad (1)$$

where $I(R,\psi,Z)$ is the intensity diffracted from a single crystallite, $\langle\ \rangle_d$ denotes averaging over all states of disorder, $\langle\ \rangle_\psi$ denotes cylindrical averaging, and c is the axial repeat distance of the molecules. The problem is then one of constructing appropriate models of a disordered crystallite and evaluating the averages in eq. (1). We have considered two different kinds of models; one of *uncorrelated* disorder, and the other of *correlated* disorder.

Uncorrelated disorder

In the case of uncorrelated disorder, for the lattice disorder we assume Gaussian statistics, that the components of the distortion vectors are independent, and that the variances of components in the 'lateral' plane (normal to the fibre axis) are equal. The cylindrically averaged diffracted intensity can then be expressed as the sum of Bragg (B) and diffuse (D) or continuous components [3,4]:

$$I_l(R) = I_l^B(R) + I_l^D(R) \qquad (2)$$

The Bragg component consists of sharp reflections whose widths (shapes) depend on the average crystallite size (as well as instrumental effects) and are constant throughout reciprocal space. As a result of the disorder, the magnitude of the Bragg reflections is weighted down with increasing resolution, the weighting function being given by [4]

$$W_{lattice}(R, Z) = \exp\left(-4\pi^2\left[R^2\sigma^2_{lat} + Z^2\sigma^2_{axial}\right]\right) \qquad (3)$$

where σ^2_{lat} and σ^2_{axial} are the variances of the lateral and axial distortions, respectively. The diffuse component consists of the continuous layer line diffraction that would be diffracted by a noncrystalline fibre except that, as a result of the disorder, it is weighted up (by $[1\text{-}w_{lattice}(R,Z)]$) with increasing resolution. The effect of substitution disorder is to weight the different Fourier-Bessel structure factors, $G_{nl}(R)$, by the weighting function

$$W_{nl} = \int_0^{c/u}\int_0^{2\pi} p(\phi, z)\exp\left[i(2\pi z l/c - n\phi)\right]d\phi dz \qquad (4)$$

where $p(\phi,z)$ is the probability density function for the angular position of a molecule deviating by ϕ, and the axial position deviating by z, from their values in an ordered lattice [4]. A particular kind of disorder is described by a particular $p(\phi,z)$ from which the w_{nl} can be calculated [4]. The effect of rotational disorder is to weight down the contribution of the higher order Fourier-Bessel terms to the Bragg intensity, and to correspondingly increase their

contribution to the diffuse intensity. The larger the variance of the rotational disorder, the more rapidly the weights fall off with Bessel order. For *random rotations*, only the zero-order Bessel term contributes to the Bragg intensity and the non-zero orders contribute to the diffuse intensity. For specimens in which the molecules are *screw disordered* (*i.e.* rotational disorder is coupled to translational disorder), for an integral helix, the contribution of a Fourier-Bessel term to the Bragg intensity is weighted down more with increasing difference between the Bessel order and the layer line index, and the contribution to the diffuse intensity is correspondingly weighted up [4].

The effects of uncorrelated disorder are illustrated in figure 1 which shows the layer line amplitudes $I_l^{1/2}(R)$ for random screw disorder, (a) alone and (b) with lattice disorder, for a molecule with 10-fold helix symmetry [4]. In (a) Bragg reflections are eliminated close to the meridian on the higher layer lines, but persist out to high resolution on all layer lines. The effect of adding lattice disorder is to suppress the Bragg reflections at high resolution as shown in (b). Note the importance of the lattice disorder in suppressing the Bragg reflections at high resolution, a feature that cannot be explained by screw disorder alone.

By calculating diffraction patterns using a molecular structure and the model of disorder described above, and comparing them with measured diffraction patterns, the disorder parameters may be adjusted, in

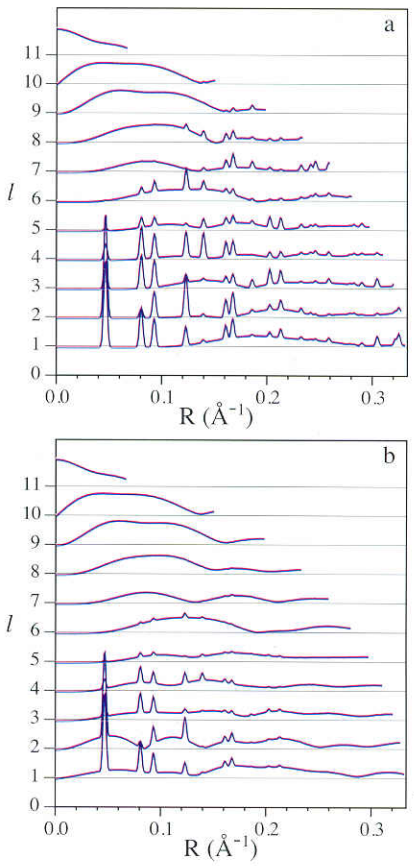

Figure 1: Calculated layer line amplitudes for a polycrystalline fibre with random screw disorder with (a) no lattice disorder and (b) uncorrelated lattice disorder [4].

an iterative fashion, to optimise the agreement between the calculated and measured patterns [5]. This allows one to identify the kind and degree of disorder in a particular fibre specimen. An example is shown in figure 2 [5]. One quadrant of a diffraction pattern recorded from a polynucleotide (poly(dA)·poly(dT)) fibre is shown in (a), and that calculated from an optimised model (including the effects of coherence length, crystallite size and disorientation) is shown in (b). The resulting model

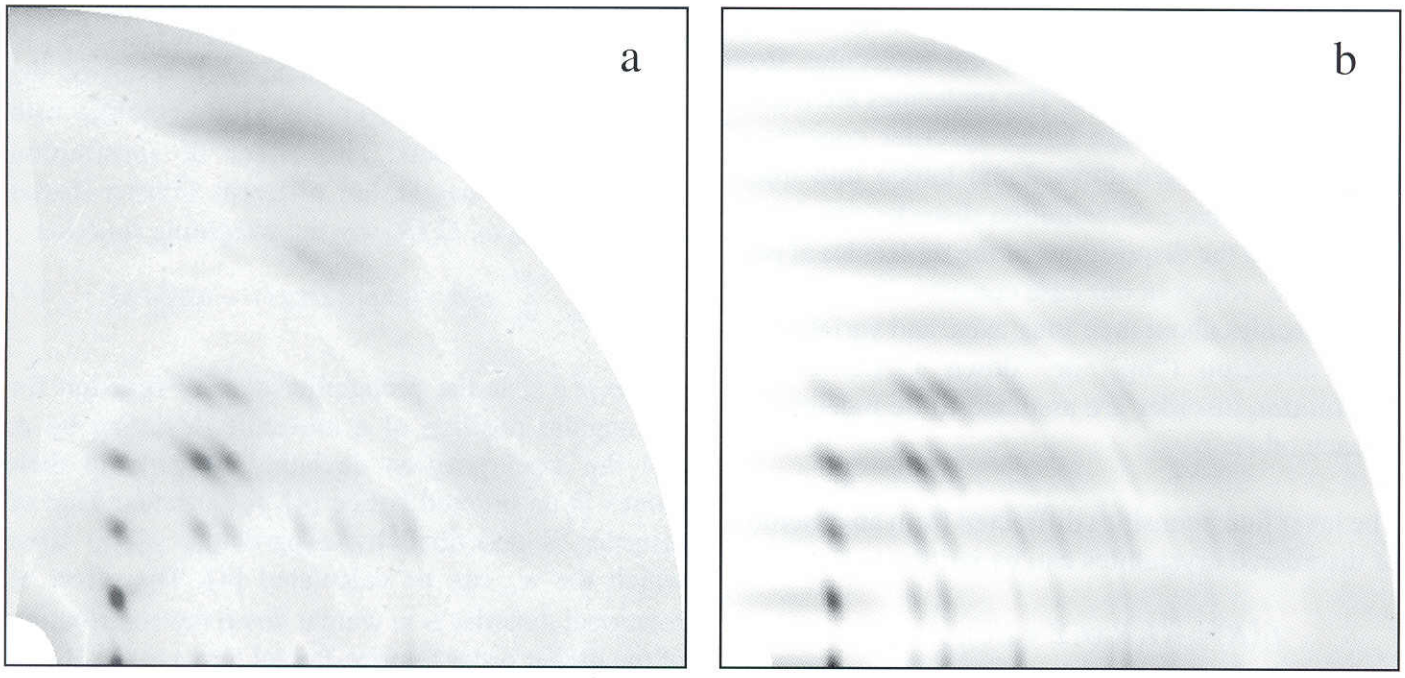

Figure 2: (a) Measured and (b) calculated (with uncorrelated disorder) diffraction patterns, in one quadrant of reciprocal space from a (poly(dA)·poly(dT)) fibre [5].

incorporates random screw disorder and lattice distortions with standard deviations of 0.6Å^{-1} along the molecular axes and 0.5Å^{-1} normal to the molecular axes.

Correlated disorder

In a close-packed system such as a crystallite in a polymer fibre, it is probable that distortions at one lattice site will influence the distortions at neighbouring sites. Furthermore, diffraction patterns from some disordered fibres do not appear to consist of distinct Bragg and diffuse components as described above, but contain Bragg reflections that broaden with increasing resolution and blend into the continuous diffraction at high resolution. This is generally considered to result from correlated distortions of the crystal lattice [8,9]. Although there may be correlations between the rotational distortions of neighbouring molecules, these are likely to be weaker and not of a general, simple form. The second model we consider therefore, is one of correlated lattice disorder and uncorrelated substitution disorder. Although the paracrystalline model is often used to describe correlated disorder in polymer crystals [8], we have chosen to use a perturbed lattice model [9] to avoid some of the difficulties inherent in the paracrystalline model[6,7]. We impose a correlation field on the crystal lattice, rather than deriving the correlations from nearest neighbour statistics, as this allows manageable expressions for calculating diffraction patterns to be obtained [6,7].

For the lattice disorder, the components of the distortion vectors are as described above, except that the distortions at neighbouring sites are coupled, the coupling being described by two exponential correlation fields, one for the lateral distortions and one for the axial distortions. The disorder is then described by lateral and axial variances, and lateral and axial correlation lengths. The degree of order in the lattice decreases as the variance increases, and increases as the correlation length increases. Uncorrelated substitution disorder (as described above) can be incorporated using the weights w_{nl}. Because of the correlations, the diffracted intensity does not separate into two components as in eq. (2), and it is not possible to express it in terms of only reciprocal space quantities. The diffracted intensity must be expressed as a sum over the real space lattice, although considerable analytical simplification is possible that allows efficient computation of the cylindrically averaged intensity

$$I_l(R) = \sum_j w_{jl}\left(R, r_j\right) \sum_{m,n} H_{mnl}\left(R, r_j, \phi_j\right) \qquad (5)$$

[6,7]. The result can be expressed in the form where the sum over j is over the sites of the undistorted two-dimensional lattice within the region of the autocorrelation function of the crystallite, the (r_j,ϕ_j) are the polar coordinates of these sites, the w_{jl} depend on the site variances and correlation lengths, the sum over m and n is over the orders of the contributing Bessel terms, and the H_{mnl} depend on the substitution disorder weights and Fourier-Bessel structure factors [6,7].

Figure 3 shows calculated diffraction patterns that illustrate the effects of correlated lattice disorder for a molecule with 11-fold helix symmetry [7]. The pattern shown in (a) is for a fibre with uncorrelated axial lattice disorder only, which has the effect of introducing diffuse intensity on the upper layer lines

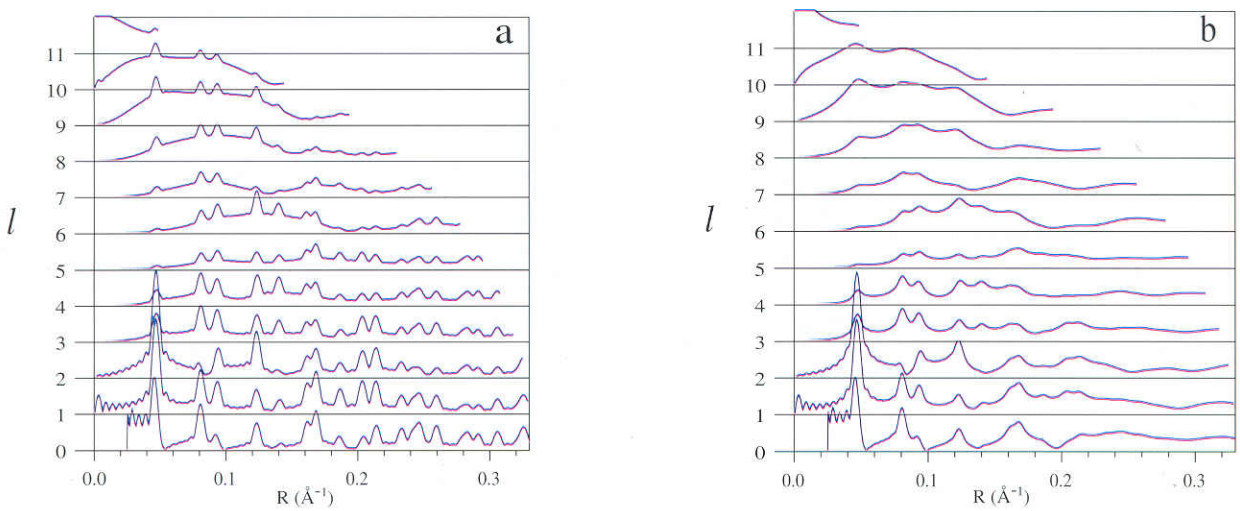

Figure 3: Calculated layer line amplitudes for a polycrystalline fibre with (a) uncorrelated axial lattice disorder, and (b) correlated lateral and axial lattice disorder [7].

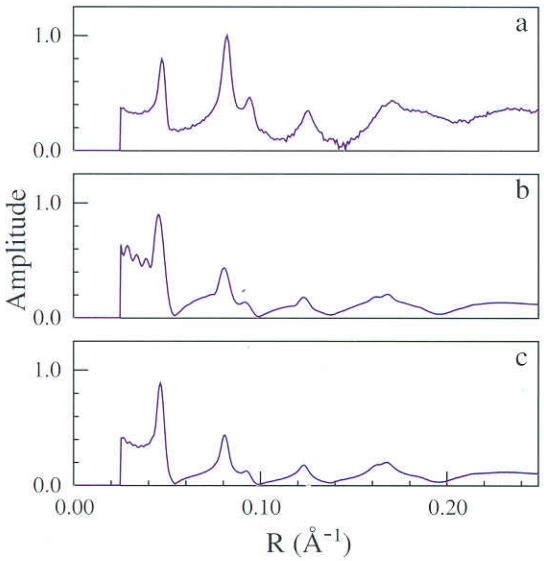

Figure 4: Equatorial diffracted amplitude, (a) measured from a (poly(dA)·poly(rU)) fibre, (b) calculated for uncorrelated disorder, and (c) calculated for correlated disorder [7].

with superimposed Bragg reflections of invariant width. The pattern in (b) shows the effects of correlated lateral and axial lattice disorder; the Bragg peaks broaden with increasing resolution and blend into the diffuse diffraction, and the pattern no longer has the appearance of a Bragg component superimposed on a continuous component.

As in the case of correlated disorder, comparison of diffraction patterns calculated using the model of correlated disorder with measured patterns may be used to characterise correlated disorder in a fibre specimen. Figure 4 shows the results of such a calculation [7]. The diffraction pattern from a polynucleotide (poly(dA)·poly(rU)) fibre shows evidence of correlated lateral lattice disorder since the Bragg reflections on the equator broaden and give way to continuous amplitude with increasing resolution (a). The best fit to the measured equatorial diffraction using a model of uncorrelated disorder (corrected for the effects of disorientation, coherence length, and instrumental broadening) is shown in (b). Although the calculated pattern matches most of the features of the observed pattern, it produces shoulders on the Bragg reflections, and Bragg reflections of constant width, neither of which are consistent with the data, and both indicating the presence of correlated disorder. A diffraction pattern calculated from an optimised model containing correlated lateral lattice disorder is shown in (c), and is seen to significantly reduce the discrepancies noted above. In this case, the lateral variance and correlation length are 1.9Å and 125Å, respectively.

Conclusions

We have developed two rather general models of disordered polycrystalline fibres that allow efficient calculation of diffraction patterns. The model of uncorrelated lattice disorder and uncorrelated substitution disorder is formulated in reciprocal space and appears to explain most of the features seen in diffraction patterns from some disordered fibres. The second model includes correlated lattice distortions (which are expected to be present to at least some degree), is formulated in real space, and appears to explain peak broadening seen in diffraction patterns from some fibres. Both models are quite flexible, and parameters describing the disorder can be adjusted to optimise the models against fibre diffraction data.

Supported by the U.S. National Science Foundation (MCB-9219736)

References

[1] A. Miller and D.A.D. Parry, A review of statistical structures in polypeptides and biological macromolecules, *Polymer*, **15**, 706-712 (1974).

[2] S. Arnott, Twenty years hard labour as a fibre diffractionist, in *Fibre Diffraction Methods*, A.D. French and K.H. Gardner (eds.), ACS Symposium Series, Vol. 141, 1- 30, 1980.

[3] R.P. Millane and W.J. Stroud, Effects of disorder on fibre diffraction patterns, *Int. J. Biol. Macromol.*, **13**, 202-208 (1991).

[4] W.J. Stroud and R.P. Millane, Diffraction by disordered polycrystalline fibres, *Acta Cryst.*, **A51**, 771-790 (1995).

[5] W.J. Stroud and R.P. Millane, Analysis of disorder in biopolymer fibres, *Acta Cryst.*, **A51**, 790-800 (1995).

[6] W.J. Stroud and R.P. Millane, Cylindrically averaged diffraction by distorted lattices, *Proc. R. Soc. Lond.*, **A452**, 151-173 (1996).

[7] W.J. Stroud and R.P. Millane, Diffraction by polycrystalline fibres with correlated disorder, *Acta Cryst.*, **A52**, 812-829 (1996).

[8] R. Hosemann and S.N. Bagchi, *Direct Analysis of Diffraction by Matter*, North-Holland, Amsterdam, 1962.

[9] T.R. Welberry, Diffuse X-ray scattering and models of disorder, *Rep. Prog. Phys.*, **48**, 1543-1593 (1985).